Single-photon generation by pulsed laser in optomechanical system via photon blockade effect

Liu Qiu, Lin Gan, Wei Ding, and Zhi-Yuan Li*

Laboratory of Optical Physics, Institute of Physics, Chinese Academy of Sciences, Beijing 100190, China
**Corresponding author: lizy@aphy.iphy.ac.cn*

Received February 25, 2013; accepted April 24, 2013;
posted May 2, 2013 (Doc. ID 185940); published May 27, 2013

We theoretically analyzed the photon quantum statistics properties of the output field from an optomechanical system driven by different pulsed lasers. Our results show that the probability of generating a single-photon state at the photon blockade region is greatly dependent on properties such as the shape, area, central frequency, length, and amplitude of the driving pulse. These results will give guidance to the design of the potential optimal optical pulse for generating a high-performance single-photon source.

OCIS codes: (270.5290) Photon statistics; (120.4880) Optomechanics.
http://dx.doi.org/10.1364/JOSAB.30.001683

1. INTRODUCTION

A single photon is among the most indispensable elements for quantum optics, quantum cryptography, communications, and computing [1–4]. One way to generate a single-photon source is to attenuate the coherent laser beams. Although the probability of obtaining the multiphoton state is reduced, the probability of obtaining the vacuum state is also increased as a result of the process, which leads to no photon being in the light source for most of the time. For an ideal single-photon source, both the vacuum state and the multiphoton state should be suppressed. Recent progress in the fabrication, manipulation, and characterization of individual nano-objects has opened new routes in the production of single-photon states [5,6]. One promising mechanism for single-photon generation is the photon blockade effect, which has been both proposed and demonstrated in the cavity quantum electrodynamics (CQED) system [7–13]. The excitation of the strong coupling CQED system by a single photon prevents subsequent photons from entering the cavity, which alters the quantum photon statistics of a light beam from random fluctuation to more orderly photon stream due to the optical nonlinearity. This strong nonlinearity at the single-photon level in the CQED system results from the strong dipole coupling between the cavity field and the two-level atom, which clearly exhibits the Jaynes–Cummings (J-C) ladder in the dressed state picture [10,14].

Recently, the photon–phonon interaction in the optomechanical system (OMS) due to the radiation pressure coupling between the mechanical motion and the photon has attracted a lot of attention [15–17]. It has been investigated for mechanical cooling [18–20], optomechanically induced transparency [21,22], and quantum sensing [23–25]. Meanwhile, researchers have been trying to push the OMS from weak optomechanical coupling to the strong coupling region at the single-photon level [18,26]. Recent theoretical study of the quantum photon statistics property and photon blockade effect in OMS has shown that the nonlinearity in OMS at the single-photon level could be used to generate a single-photon state at the strong optomechanical coupling region [27]. By using a two-mode OMS, the nonlinearity could be enhanced [28]. However, for single-photon resource application, the source must be operated in a pulsed region. This raises the prospect for possible modulation of the single-photon state at a single pulse region. This problem has still not been studied, although researchers have used different optical pulses for cooling and the entanglement generation in OMS [29–31].

In this work, we studied nonclassical photon-state generation by pulsed-laser-driven OMS via the photon blockade effect in the strong optomechanical coupling region. We analyzed the different parameters for the pulse to generate a single-photon state in OMS. This article is organized as follows. In Section 2, the setup and the model Hamiltonian are introduced. In Section 3, we analyze the quantum photon statistics property of the output field from OMS driven by a Gaussian pulse. In Section 4, we compare the other two configurations of the pulse shape. Finally, the experimental results and the conclusion are given in Section 5.

2. PHOTON BLOCKADE IN OPTOMECHANICAL SYSTEM

We considered the setup as schematically shown in Fig. 1. A cavity with an oscillating mirror at one end is coherently driven by a weak pulsed-laser field, which leads to modulation of the optical cavity mode by motion of the mechanical oscillator. In a frame rotating with the laser frequency ω_l, under the rotating wave approximation, the Hamiltonian of this system can be written as

$$H(t) = \hbar(\omega_c - \omega_l)a^+a + \hbar\omega_m b^+b + \hbar G a^+a(b^+ + b) + i\hbar E(t)(a^+ - a), \quad (1)$$

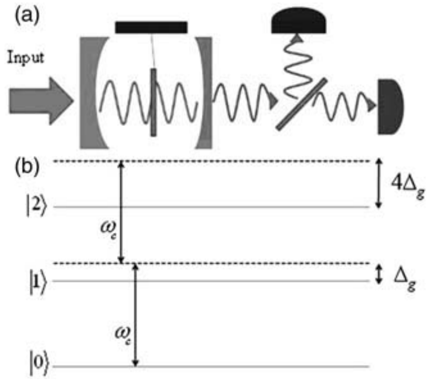

Fig. 1. (a) Schematic for the setup. (b) Level diagram of different photon states for single-mode OMS.

where $a(b)$ is the bosonic annihilation operator of the single-mode cavity (mechanical) mode with resonant frequency ω_c (ω_m), G is the single-photon optomechanical coupling efficiency, and $E(t)$ is the strength of the driving laser. To describe the loss of the system, two dissipation channels are usually taken into consideration, the optical cavity field decay characterized by photon decay rates κ and the mechanical damping with rate γ.

In CQED systems, the strong coupling between the atom and photons leads to the famous J-C ladder. Meanwhile, in OMS, due to the radiation pressure force, the resonator equilibrium is shifted with a quantity proportional to the photon number n_c for the photon number state $|n_c\rangle$. This leads to a decrease of the state energy of the photon state $|n_c\rangle$ by $n_c^2 \times \Delta_g$, where $\Delta_g = g_0^2/\omega_m$ [27]. As a result, this modulation to the energy of the photon number state leads to a different resonance requirement for the first and multiple photons excited in the cavity. The energy displacement gives rise to nonlinear optical phenomena at the single-photon level in OMS. One of these is the photon blockade effect, where strong optomechanical interaction prevents multiple photons from entering the cavity at the same time. For example, in OMS driven by a coherent laser, if a single photon is coupled to the excited state $|1\rangle$ with energy $\omega_c - \Delta_g$, the coupling of another photon with energy $\omega_c - \Delta_g$ will not make the transition to the photon state $|2\rangle$, which actually requires energy $\omega_c - 3\Delta_g$. As a result, the probability of coupling the second photon into the OMS is greatly reduced due to the strong optomechanical coupling.

This nonlinearity in the OMS system could be used to generate a single-photon source. As depicted in Fig. 1, the input light is coupled into the cavity and collected at the output port. To generate a practical single-photon source, the output is required to be deterministic. The optomechanical interaction is required to be controlled in the time domain. For this reason, one needs to drive the OMS with a controllable light pulse with certain parameters.

To study the photon statistics property of the output field, we adopted the quantum trajectory method (QTM) to obtain the photon distribution. In the quantum Monte Carlo simulation according to QTM, the Schrodinger equation is written as

$$i\frac{\partial\psi}{\partial t} = H_{\text{eff}}(t)\psi, \tag{2}$$

where $H_{\text{eff}}(t)$ is given by

$$H_{\text{eff}}(t) = H(t) - \frac{i}{2}\sum_{i=1} d_i D_i^+ D_i, \tag{3}$$

in which D_i and d_i indicate the collapse operator and dissipation rate of the dissipation channel of the system, and $H(t)$ is the Hamiltonian of the system without consideration of the loss. Compared to the mechanical dissipation, the cavity decay is dominant if the OMS is put in a cryostat environment to reduce the mechanical decoherence caused by the thermal surroundings. For simplicity, we only take the cavity decay into consideration, and the output field is monitored to yield information about the cavity decay.

3. OMS DRIVEN BY COHERENT GAUSSIAN PULSE

Generally, the input laser pulse could be of any specific shape. We first studied the OMS driven by coherent Gaussian pulses, with controllable pulse parameters such as duration, amplitude, and central frequency. In our simulation, $E(t)$ in Eq. (1) is given by the form $E(t) = E_0 p(t)$, where E_0 is the amplitude and $p(t)$ is the time dependence of the pulse, which is given as

$$p(t) = \exp\left[-\left(\frac{t - t_0}{\tau}\right)^2\right], \tag{4}$$

where t_0 is the pulse center and τ is the pulse length. Each laser pulse was coupled into the cavity, and the histogram of the collected photons was made to analyze the photon distribution of the output field. Generally, the output field is not an ideal single-photon source, and it could be expanded in the Fock state basis, which can be written as

$$|\text{out}\rangle = \sum_{n=0}^{\infty} \alpha_n |n\rangle, \tag{5}$$

where α_n is the probability for the photon state $|n\rangle$. The normalized value $|p(n)|^2 = |\alpha_n|^2/\sum_i |\alpha_i|^2$ could be estimated from the number of detected photons at the output when running a large number of trajectories. We can make histogram of how many photons we detect and perform a statistical measurement on the trajectories. For example, $|p(n)|^2$ could be estimated from the relative number of trajectories for which n counts were detected at the output. In this case, if the desired output state is nearly a single-photon state, we should change the parameters of system to optimize the $|p(1)|^2$ to its maximum.

Firstly, we analyze the OMS with mechanical mode $\omega_m = 2\pi \times 10$ MHz, optomechanical coupling $G = 0.6\omega_m$, and cavity decay $\kappa = 0.025\omega_m$ driven by a Gaussian pulsed laser with amplitude $E = \kappa$ and pulse length $0.4/\kappa$. In Fig. 2, the probabilities of the zero-photon, single-photon, and multiple-photon states versus the central frequency of the driving pulse are presented with detection after a number of quantum trajectories. The maximum probability of the single-photon state generated from the recorded output field is 0.55 at the frequency $-0.36\omega_m$. This corresponds well to the theoretical predicted result $-\Delta_g = -G^2/\omega_m$, which meets the condition in which κ is smaller than ω_m and G for an OMS weakly driven by a continuous coherent laser.

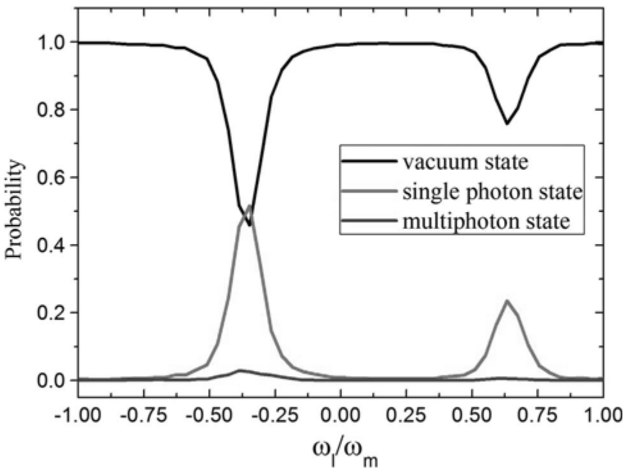

Fig. 2. Probabilities of different photon states versus the central frequency of the driving pulse in OMS with $\omega_m = 2\pi \times 10$ MHz, $\kappa = 0.025\omega_m$, $\tau = 0.4/\kappa$, $G = 0.6\omega_m$, and $\tau = 0.4/\kappa$.

As a result, we set the central frequency of the coherent driving laser to $\omega_0 - \Delta_g$, and analyzed the photon distribution of the output field under different amplitudes of the driving pulse. As shown in Fig. 3(a), the probability of the single-photon state in the output field, having a maximum value 0.765, shows an oscillation with respect to the intensity of the driving field with an approximate period of 4κ. This feature is similar to the result in the Gaussian-pulse-driven CQED system [32]. The blocking of the second photon into the cavity is greatly dependent on the existence of the first photon in OMS.

For comparison, we analyzed an OMS in a weaker coupling region with mechanical mode $\omega_m = 2\pi \times 10$ MHz, optomechanical coupling $G = 0.1\omega_m$, and cavity decay $\kappa = 0.025\omega_m$ under the same driven condition. As presented in Fig. 3(b), there is no such oscillation. The probability of single-photon state reaches its maximum value 0.35, which is lower than the value in the strong coupling region, and quickly decreases as the intensity of the driving pulse increases, while the coefficient of the multiphoton state increases to 1. It is easy to understand that in this weaker coupling region the input laser pulse goes through the cavity decay channel without adequate optomechanical interaction. For OMS with $\omega_m = 2\pi \times 10$ MHz, $G = 0.1\omega_m$, and $\kappa = 0.025\omega_m$, when we fixed the driving amplitude to 2κ and changed the pulsewidth, there was also an oscillation in the probability for a single-photon state, as shown in Fig. 3(c). The maximum probability of a single-photon state is now 0.78 at a driving amplitude of $0.412/\kappa$.

Another statistical property to characterize the light field is second-order correlation. For an ideal single-photon source, the zero-time delay second-order correlation $g^{(2)}(0)$ is 0, which means that the possibility of coexistence of two photons emitting at the same time from the output is zero. Given the probability α_n of photon state $|n\rangle$, one can easily obtain the zero-time delay second-order correlation, which could be written as

$$g^{(2)}(0) = \frac{\langle a^+ a^+ a a\rangle}{\langle a^+ a\rangle^2} = \frac{\sum_{n=0}^{\infty} n(n-1)|\alpha_n|^2}{\left(\sum_{n=0}^{\infty} n|\alpha_n|^2\right)^2}. \quad (6)$$

For the strong coupling case discussed above, $g^{(2)}(0)$ is presented in Fig. 4(a). $g^{(2)}(0)$ is almost zero when the driving amplitude is small. At the strong coupling region for continuous coherent driving OMS, the theoretical minimum value for $g^{(2)}(0)$ is

$$\frac{\kappa^2}{\omega_m^2}\left[\frac{1}{\eta^4} + \frac{4\eta^4}{(\kappa/\omega_m)^2 + (1-2\eta^2)^2}\right], \quad (7)$$

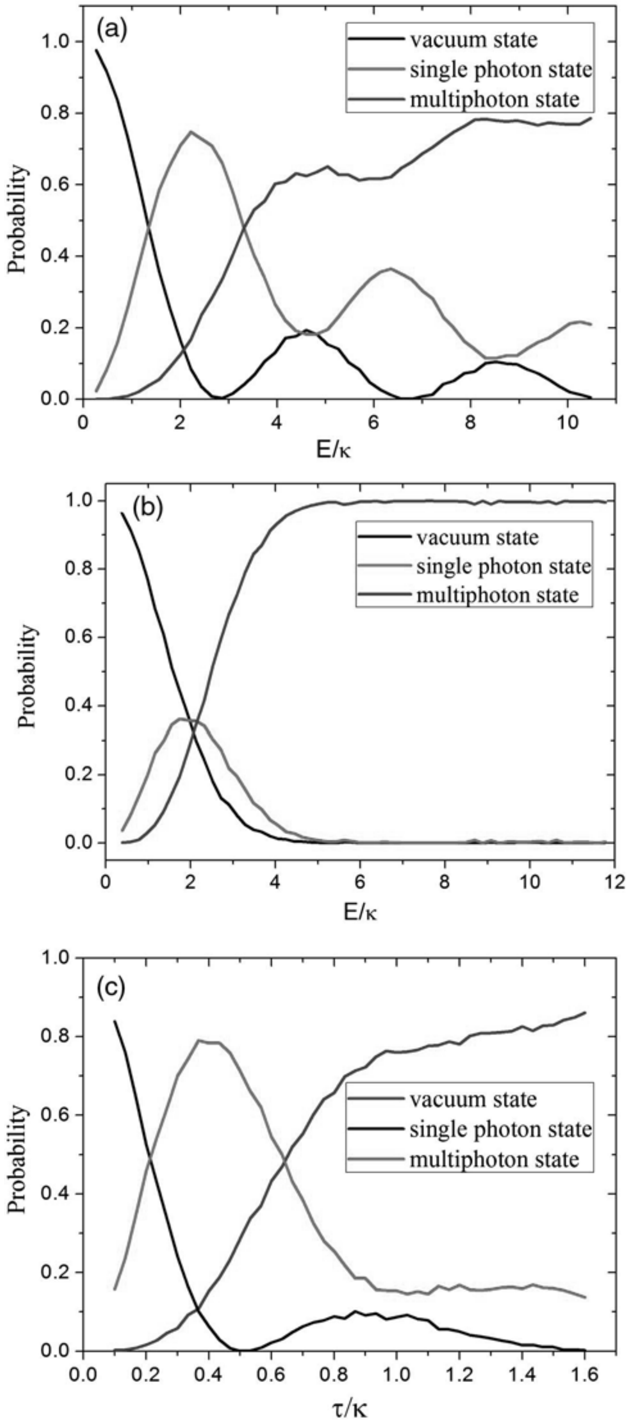

Fig. 3. Probabilities of different photon states versus (a),(b) amplitude and (c) length of the driving pulse. (a) is for $\omega_m = 2\pi \times 10$ MHz, $\kappa = 0.025\omega_m$, $\tau = 0.4/\kappa$, and $G = 0.6\omega_m$; (b) is for $\omega_m = 2\pi \times 10$ MHz, $\kappa = 0.025\omega_m$, $\tau = 0.4/\kappa$, and $G = 0.1\omega_m$; and (c) is for $\omega_m = 2\pi \times 10$ MHz, $\kappa = 0.025\omega_m$, $E = 2\kappa$, and $G = 0.6\omega_m$.

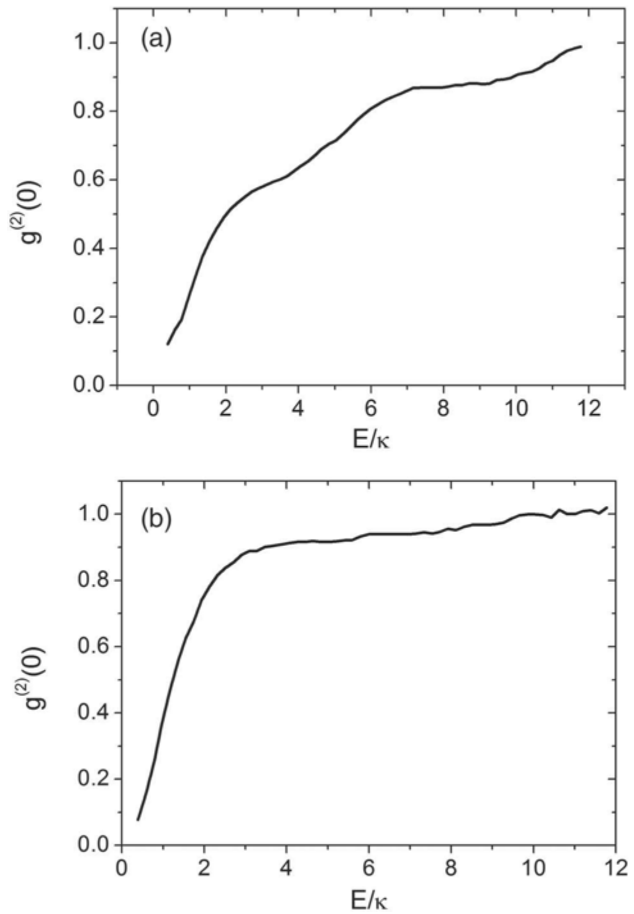

Fig. 4. Zero-time delay second-order correlation function versus amplitude of the driving pulse with parameters of (a) $\omega_m = 2\pi \times 10$ MHz, $\kappa = 0.025\omega_m$, $\tau = 0.4/\kappa$, and $G = 0.6\omega_m$, and (b) $\omega_m = 2\pi \times 10$ MHz, $\kappa = 0.025\omega_m$, $\tau = 0.4/\kappa$, and $G = 0.1\omega_m$.

where $\eta = g_0/\omega_m$. As we can see, when OMS is driven by the pulsed laser, the minimum value of $g^{(2)}(0)$ is almost zero. As a comparison, the minimum value of $g^{(2)}(0)$ is 0.009 when OMS is driven by continuous coherent laser. As shown in Fig. 4, there is an oscillation in the slope of the zero-time delay second-order function for the strong coupling case [Fig. 4(a)], while no oscillation appears in the weak coupling case [Fig. 4(b)].

4. OMS DRIVEN BY RECTANGULAR AND SINE PULSES

For comparison, we further analyzed the OMS driven by sine and rectangular pulses. For both pulses, the OMS has the same parameters as the stronger coupling case mentioned above. For the sine pulse, we set the period to $\sqrt{2\pi} \times 0.8/\kappa$, which leads to the same pulse area and the same maximum value with the Gaussian pulse under the same driving amplitude. The output photon distribution as a function of the intensity of the driving laser pulse is presented in Fig. 5(a). From the quantum statistics of the output field, we could clearly see an oscillation in the probabilities for different photon states with the increase of the strength of the driving pulse. The probability for generating a single-photon state reaches its peak value of 0.78 at the driving amplitude of 2.1κ. In comparison to the results shown in Fig. 3(a), the chances of preventing multiphoton states are almost the same. Besides, the oscillatory period for the amplitude here is almost 4κ, which is also the same as the Gaussian

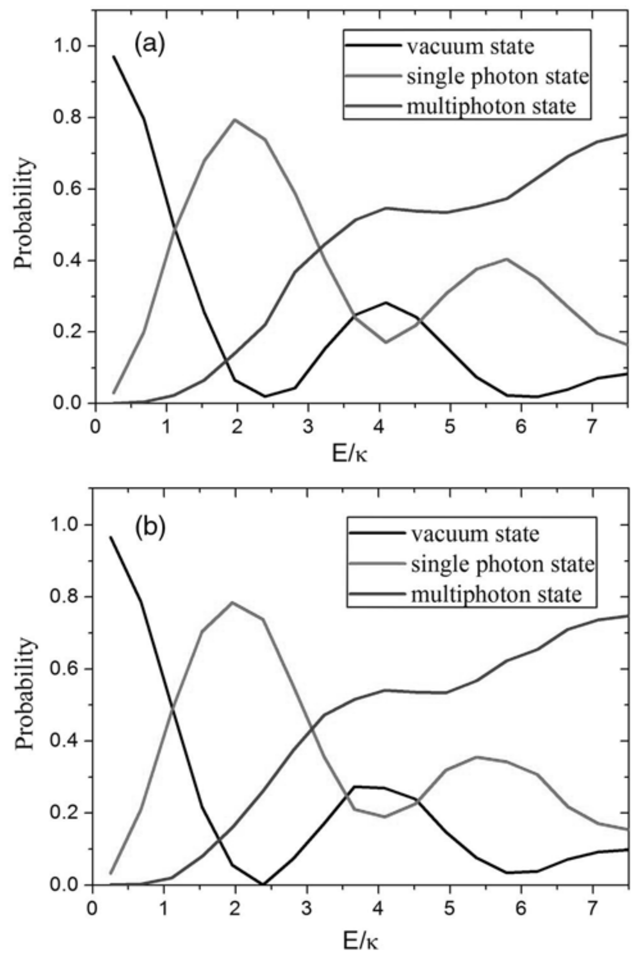

Fig. 5. Probabilities of different photon states versus driving pulse with different wave shapes: (a) sine shape and (b) rectangular shape.

laser pulse. For the rectangular pulse as depicted in Fig. 5(b), we set the pulsewidth to $\sqrt{2\pi} \times 0.4/\kappa$, which also has the same pulse area and the same maximum value with the Gaussian pulse under the same driving amplitude. The photon distribution as a function of driving strength is presented in Fig. 5(b). It shows that the probabilities of obtaining different photon states are almost the same. This indicates that under the same driving amplitude for a laser pulse with the same pulse area, the chances for coupling of photons in the OMS are the same.

5. CONCLUSION

Strong single-photon optomechanical coupling has been demonstrated in a cold atoms system in which the collective motion of atoms plays the mechanical role [33,34]. However, it still has not been achieved in a solid-state system. Equipped with cryostat facilities at ultralow temperature to reduce the mechanical decoherence rate, fast developments in nanofabrication and structure design are expected to lead the OMS to the strong coupling region. In the OMS that we studied at the strong coupling region, the frequency of the mechanical mode is $2\pi \times 10$ MHz, the cavity decay rate is $2\pi \times 0.25$ MHz, and the pulse length is at the scale of several microseconds. Compared with the optimal Gaussian pulse length in the CQED system, which is usually around nanoseconds, it is more controllable to design the possible optimal optical pulse in the OMS system, which is an advantage of the single-photon source in the CQED system.

In summary, we have theoretically analyzed the photon statistics property of the output field from OMS driven by pulsed lasers of different temporal profiles. The probability of generating a single-photon state at the photon blockade region is greatly dependent on properties such as shape, central frequency, length, and the amplitude of the driving pulse. It will give us guidance to design the potential optimal optical pulse for generating a single-photon source, which is a very important quantity for quantum key distribution, quantum repeaters, and photonic quantum information processing and quantum simulation [2,4,35,36].

ACKNOWLEDGMENTS

This work was supported by the National Basic Research Foundation of China under grant No. 2011CB922002, and the Knowledge Innovation Program of the Chinese Academy of Sciences (No. Y1V2013L11).

REFERENCES

1. L. M. Duan and H. J. Kimble, "Scalable photonic quantum computation through cavity-assisted interactions," Phys. Rev. Lett. **92**, 127902 (2004).
2. E. Knill, R. Laflamme, and G. J. Milburn, "A scheme for efficient quantum computation with linear optics," Nature **409**, 46–52 (2001).
3. L. Childress, J. M. Taylor, A. S. Sorensen, and M. D. Lukin, "Fault-tolerant quantum repeaters with minimal physical resources and implementations based on single-photon emitters," Phys. Rev. A **72**, 052330 (2005).
4. T. D. Ladd, P. van Loock, K. Nemoto, W. J. Munro, and Y. Yamamoto, "Hybrid quantum repeater based on dispersive CQED interactions between matter qubits and bright coherent light," New J. Phys. **8**, 184 (2006).
5. B. Lounis and M. Orrit, "Single-photon sources," Rep. Prog. Phys. **68**, 1129–1179 (2005).
6. G. S. Solomon, E. B. Flagg, S. V. Polyakov, T. Thomay, and A. Muller, "Manipulating single photons from disparate quantum sources to be indistinguishable [Invited]," J. Opt. Soc. Am. B **29**, 319–327 (2012).
7. A. Imamoglu, H. Schmidt, G. Woods, and M. Deutsch, "Strongly interacting photons in a nonlinear cavity," Phys. Rev. Lett. **79**, 1467–1470 (1997).
8. L. Schneebeli, M. Kira, and S. W. Koch, "Characterization of strong light-matter coupling in semiconductor quantum-dot microcavities via photon-statistics spectroscopy," Phys. Rev. Lett. **101**, 097401 (2008).
9. I. Schuster, A. Kubanek, A. Fuhrmanek, T. Puppe, P. W. H. Pinkse, K. Murr, and G. Rempe, "Nonlinear spectroscopy of photons bound to one atom," Nat. Phys. **4**, 382–385 (2008).
10. K. M. Birnbaum, A. Boca, R. Miller, A. D. Boozer, T. E. Northup, and H. J. Kimble, "Photon blockade in an optical cavity with one trapped atom," Nature **436**, 87–90 (2005).
11. A. Ridolfo, M. Leib, S. Savasta, and M. J. Hartmann, "Photon blockade in the ultrastrong coupling regime," Phys. Rev. Lett. **109**, 193602 (2012).
12. A. Majumdar, M. Bajcsy, A. Rundquist, and J. Vučković, "Loss-enabled sub-Poissonian light generation in a bimodal nanocavity," Phys. Rev. Lett. **108**, 183601 (2012).
13. D. Press, S. Gotzinger, S. Reitzenstein, C. Hofmann, A. Loffler, M. Kamp, A. Forchel, and Y. Yamamoto, "Photon antibunching from a single quantum-dot-microcavity system in the strong coupling regime," Phys. Rev. Lett. **98**, 117402 (2007).
14. A. Majumdar, M. Bajcsy, and J. Vuckovic, "Probing the ladder of dressed states and nonclassical light generation in quantum-dot-cavity QED," Phys. Rev. A **85**, 041801 (2012).
15. T. J. Kippenberg and K. J. Vahala, "Cavity optomechanics: back-action at the mesoscale," Science **321**, 1172–1176 (2008).
16. M. Aspelmeyer, P. Meystre, and K. Schwab, "Quantum optomechanics," Phys. Today **65**(7), 29–35 (2012).
17. M. Aspelmeyer, S. Groblacher, K. Hammerer, and N. Kiesel, "Quantum optomechanics—throwing a glance [Invited]," J. Opt. Soc. Am. B **27**, A189–A197 (2010).
18. S. Groblacher, K. Hammerer, M. R. Vanner, and M. Aspelmeyer, "Observation of strong coupling between a micromechanical resonator and an optical cavity field," Nature **460**, 724–727 (2009).
19. A. Schliesser, O. Arcizet, R. Riviere, G. Anetsberger, and T. J. Kippenberg, "Resolved-sideband cooling and position measurement of a micromechanical oscillator close to the Heisenberg uncertainty limit," Nat. Phys. **5**, 509–514 (2009).
20. D. J. Wilson, C. A. Regal, S. B. Papp, and H. J. Kimble, "Cavity optomechanics with stoichiometric SiN films," Phys. Rev. Lett. **103**, 207204 (2009).
21. S. Weis, R. Riviere, S. Deleglise, E. Gavartin, O. Arcizet, A. Schliesser, and T. J. Kippenberg, "Optomechanically induced transparency," Science **330**, 1520–1523 (2010).
22. C. Jiang, B. Chen, and K. D. Zhu, "Controllable nonlinear responses in a cavity electromechanical system," J. Opt. Soc. Am. B **29**, 220–225 (2012).
23. S. Kolkowitz, A. C. Jayich, Q. P. Unterreithmeier, S. D. Bennett, P. Rabl, J. G. Harris, and M. D. Lukin, "Coherent sensing of a mechanical resonator with a single-spin qubit," Science **335**, 1603–1606 (2012).
24. M. Eichenfield, R. Camacho, J. Chan, K. J. Vahala, and O. Painter, "A picogram- and nanometre-scale photonic-crystal optomechanical cavity," Nature **459**, 550–555 (2009).
25. X. Sun, J. Zheng, M. Poot, C. W. Wong, and H. X. Tang, "Femtogram doubly clamped nanomechanical resonators embedded in a high-Q two-dimensional photonic crystal nanocavity," Nano Lett. **12**, 2299–2305 (2012).
26. P. Meystre and S. Stenholm, "The mechanical effects of light—introduction," J. Opt. Soc. Am. B **2**, 1706 (1985).
27. P. Rabl, "Photon blockade effect in optomechanical systems," Phys. Rev. Lett. **107**, 063061 (2011).
28. M. Ludwig, A. H. Safavi-Naeini, O. Painter, and F. Marquardt, "Enhanced quantum nonlinearities in a two-mode optomechanical system," Phys. Rev. Lett. **109**, 063061 (2012).
29. L. Tian and H. L. Wang, "Optical wavelength conversion of quantum states with optomechanics," Phys. Rev. A **82**, 053806 (2010).
30. J. Q. Liao and C. K. Law, "Cooling of a mirror in cavity optomechanics with a chirped pulse," Phys. Rev. A **84**, 053838 (2011).
31. M. R. Vanner, I. Pikovski, G. D. Cole, M. S. Kim, C. Brukner, K. Hammerer, G. J. Milburn, and M. Aspelmeyer, "Pulsed quantum optomechanics," Proc. Natl. Acad. Sci. USA **108**, 16182–16187 (2011).
32. A. Faraon, A. Majumdar, and J. Vučković, "Generation of nonclassical states of light via photon blockade in optical nanocavities," Phys. Rev. A **81**, 033838 (2010).
33. S. Gupta, K. L. Moore, K. W. Murch, and D. M. Stamper-Kurn, "Cavity nonlinear optics at low photon numbers from collective atomic motion," Phys. Rev. Lett. **99**, 213601 (2007).
34. F. Brennecke, S. Ritter, T. Donner, and T. Esslinger, "Cavity optomechanics with a Bose–Einstein condensate," Science **322**, 235–238 (2008).
35. S. Barz, E. Kashefi, A. Broadbent, J. F. Fitzsimons, A. Zeilinger, and P. Walther, "Demonstration of blind quantum computing," Science **335**, 303–308 (2012).
36. A. Aspuru-Guzik and P. Walther, "Photonic quantum simulators," Nat. Phys. **8**, 285–291 (2012).